

# Inhibition of *Escherichia coli* porphobilinogen synthase using analogs of postulated intermediates

Caroline Jarret, Frédéric Stauffer, Matthias E Henz, Maurus Marty, Rainer M Lüönd, Janette Bobálová, Peter Schürmann and Reinhard Neier

**Background:** Porphobilinogen synthase is the second enzyme involved in the biosynthesis of natural tetrapyrrolic compounds, and condenses two molecules of 5-aminolevulinic acid (ALA) through a nonsymmetrical pathway to form porphobilinogen. Each substrate is recognized individually at two different active site positions to be regioselectively introduced into the product. According to pulse-labeling experiments, the substrate forming the propionic acid sidechain of porphobilinogen is recognized first. Two different mechanisms for the first bond-forming step between the two substrates have been proposed. The first involves carbon–carbon bond formation (an aldol-type reaction) and the second carbon–nitrogen bond formation, leading to an iminium ion.

**Results:** With the help of kinetic studies, we determined the Michaelis constants for each substrate recognition site. These results explain the Michaelis–Menten behavior of substrate analog inhibitors – they act as competitive inhibitors. Under standard conditions, however, another set of inhibitors demonstrates uncompetitive, mixed, pure irreversible, slow-binding or even quasi-irreversible inhibition behavior.

**Conclusions:** Analysis of the different classes of inhibition behavior allowed us to make a correlation between the type of inhibition and a specific site of interaction. Analyzing the inhibition behavior of analogs of postulated intermediates strongly suggests that carbon–nitrogen bond formation occurs first.

## Introduction

Porphobilinogen synthase (PBGS, E.C. 4.2.1.24), also called 5-aminolevulinatase (ALAD), is the second enzyme in the biosynthetic pathway of the ‘pigments of life’ [1]. This enzyme catalyzes the formation of porphobilinogen (PBG; **1**; Figure 1) by a nonsymmetrical pathway starting with two identical substrates: two molecules of 5-aminolevulinic acid (ALA; **2**) [2,3]. PBG is transformed, with the help of two additional enzymes, to the last common precursor of all natural tetrapyrroles — uroporphyrinogen III [4,5]. These three initial steps are common to all organisms that synthesize tetrapyrrolic natural products. In the absence of PBGS, two molecules of ALA condense to a symmetric diimine, which is oxidized to the pyrazine **3** [6]. Under anaerobic conditions the formation of small amount of pseudo-PBG has been reported [7,8], and in the presence of Amberlite TR-45 the formation of PBG has been reported [6,7].

PBGS is a metalloenzyme that has been found in bacteria, plants, animals and humans [9]. Early on, it was recognized that the enzyme is a homo-octamer [10], and primary structures suggest that all PBGSs share a high degree of homology [11,12]. It has been shown that PBGS forms a Schiff base with at least one of the two substrates

Address: Institute of Chemistry, University of Neuchâtel, CH-2000 Neuchâtel, Switzerland.

Correspondence: Reinhard Neier  
E-mail: Reinhard.Neier@ich.unine.ch

**Key words:** analogs of intermediates, inhibition studies, porphobilinogen synthase

Received: 19 November 1999  
Revisions requested: 9 December 1999  
Revisions received: 6 January 2000  
Accepted: 13 January 2000

Published: 21 February 2000

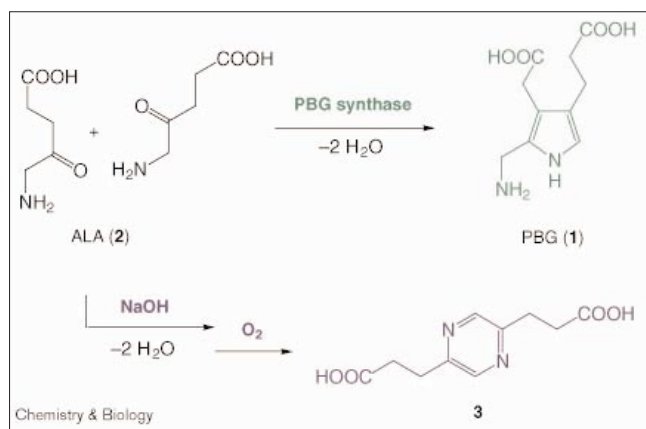
**Chemistry & Biology** 2000, 7:185–196

1074-5521/00/\$ – see front matter  
© 2000 Elsevier Science Ltd. All rights reserved.

[13]. The identification of the Schiff base as a competent intermediate in the biosynthetic pathway has strongly influenced proposals about the enzyme’s mechanism [14]. An active-site lysine residue was identified using labeled substrate, which was irreversibly bound to the enzyme by reduction with NaBH<sub>4</sub> [14]. The amino-acid sequences in the vicinity of the active-site lysine are highly conserved [15]. Also, the overall homology of the PBGS sequences from different organisms is high [12]. Studies on the influence of bivalent metal ions such as Zn<sup>2+</sup> or Mg<sup>2+</sup> on the activity of PBGSs from different sources suggested that there are different classes of PBGSs [16]. The Zn<sup>2+</sup>-enzymes contain a zinc finger rich in cysteine and histidine residues, whereas in the enzymes isolated from plants (Mg<sup>2+</sup> enzymes) an aspartate-rich region has been identified [15].

Despite intensive studies of PBGSs from different sources, the exact mechanism of PBG formation is not yet clear. High-resolution X-ray structures have been published [17–20] and gave important additional information, but some uncertainties remain. On the basis of the X-ray structure, a second lysine residue was identified that appears to be protonated and important for the Schiff base formation, and, in the Zn<sup>2+</sup> enzymes, a water molecule

Figure 1

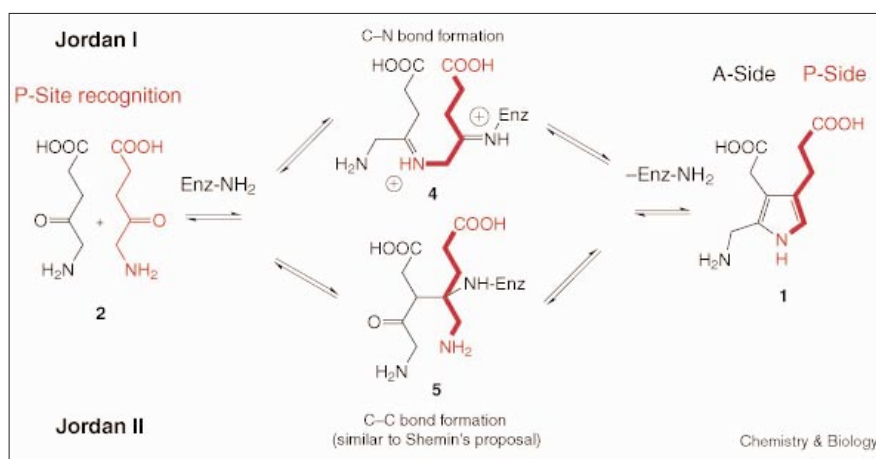


The asymmetric enzymatic synthesis of porphobilinogen (PBG) from two molecules of 5-aminolevulinic acid (ALA). The biochemical transformation corresponds to a Knorr-type pyrrole synthesis during which two molecules of  $\text{H}_2\text{O}$  are eliminated. In aqueous solution ALA is present mainly as neutral zwitterion, in contrast to the PBG product, which is negatively charged. The chemical dimerization of ALA under aerobic conditions leads to the formation of the pyrazine **3**. During this transformation two molecules of  $\text{H}_2\text{O}$  are eliminated, but the oxidation of the dihydropyrazine to the pyrazine by the formal elimination of one  $\text{H}_2$  molecule is essential to obtain the stable aromatic heterocycle **3**.

bound to a  $\text{Zn}^{2+}$  near the active site was postulated to play a significant role in the biosynthetic transformation [17]. The recently published X-ray structure of the first  $\text{Mg}^{2+}$ -containing PBGS clearly shows that  $\text{Mg}^{2+}$  plays a different role than  $\text{Zn}^{2+}$ . The  $\text{Mg}^{2+}$  is not present at the active site but is bound at the interface of the dimer. It has been suggested that  $\text{Mg}^{2+}$  exercises its allosteric rate enhancement using a structure-based mechanism [20].

Figure 2

The key steps for the enzymatic transformation of ALA to PBG. For simplicity, the two mechanisms have been designated Jordan I and Jordan II. The two substrates are identified by their position in the final PBG product. The A-side is the acetic acid sidechain of PBG (the ALA that becomes the acetic acid sidechain is recognized by the A-site of the enzyme), and the P-side is the propionic acid sidechain (the enzyme's P-site recognizes the ALA molecule that becomes the P-side of PBG). Based on Jordan's pulse-labeling experiments, the P-side substrate forms the first Michaelis–Menten complex with the enzyme. The 'first' substrate is red and all the structures derived from the P-side substrate are also red. The two mechanistic proposals for the enzymatic transformation differ in the sequence of the bond-forming steps. In one mechanism (Jordan I), the Schiff base formation is the first step that connects the two substrates (**4**). In the second



mechanism (Jordan II), which is closely related to the initial proposal of Shemin, an aldol-type reaction is postulated as the key step (**5**).

Both mechanisms had been analyzed in comparison to the two class of aldolases (aldolase I and II).

Different mechanisms have been proposed for this seemingly simple Knorr-type condensation [21]. Nandi and Shemin [14] first postulated a mechanism that is analogous to the reaction catalyzed by the class I aldolases, and this mechanism became widely accepted [22].

Several years later Jordan and Seehra [23] determined that the first ALA recognized by the enzyme forms the propionic acid sidechain in the final product (the P-side of the product is recognized by the P-site of the enzyme; Figure 2) using an elegant pulse-labeling experiment with  $[5\text{-}^{14}\text{C}]\text{ALA}$ . This finding was in contrast to the sequence of recognition events postulated by Nandi and Shemin [14]. Following Schiff base formation between the enzyme and the P-side ALA, Jordan and Seehra [23] postulated that the first connection between the P-side and the A-side ALA is formed by a carbon–nitrogen bond, leading to intermediate **4** (Figure 2). This sequence of recognition events for the two substrates, as well as the first connecting step, had already been suggested by Granick and Mauzerall [24]. A mechanistic alternative that follows more closely the second part of Nandi and Shemin's proposal [14] and involves intermediate **5** formed by an aldol type reaction was also proposed [3,5] (Figure 2). It has been difficult to prove either mechanism until now.

Our group has been investigating the mechanism of PBGS using systematic inhibition studies for several years [9,25]. To test the recognition sites of *Escherichia coli* [9] and *Rhodobacter spheroides* [25] PBGSs, a series of substrate, product and postulated intermediate analogs were synthesized and their inhibition potencies determined. The goal of these investigations was to contribute to our knowledge about the active site of the enzyme, to elucidate possible

mechanisms for the transformation and to analyze the differences between enzymes from different sources.

In recent years, several groups have contributed significantly to our knowledge in this field [26–28]. Because several recombinant enzymes are now available in large quantities, more systematic studies are possible. The behavior of the enzymes from *E. coli*, *Saccharomyces cerevisiae* and *Pisum sativum* (a plant enzyme) have been systematically compared [26]. Despite this effort, a clear answer concerning the mechanism of PBGS has not been obtained.

At some point during the PBGS-catalyzed reaction a long chain dicarboxylate intermediate is formed. Here we describe our studies on the inhibition potency of this type of compound. To try to distinguish between the two major mechanistic proposals, diacids containing seven carbon atoms (suggesting that C–C bond formation occurs first)

[5,14] or diacids containing ten carbon atoms (suggesting C–N bond formation occurs first) were used [23]. Varying the chain length should allow the importance of the exact distance between the two carboxylate ends of the molecules to be deduced.

The kinetics of PBGS are complex because this enzyme is a bisubstrate enzyme [29], and understanding the inhibition behavior of this class of enzymes is often not straightforward. The observed kinetics for PBGS under the standard assay conditions (ALA concentration between 80 and 400  $\mu\text{M}$ ), however, must follow the laws of a Michaelis–Menten kinetics [30] (Figure 3a).

## Results

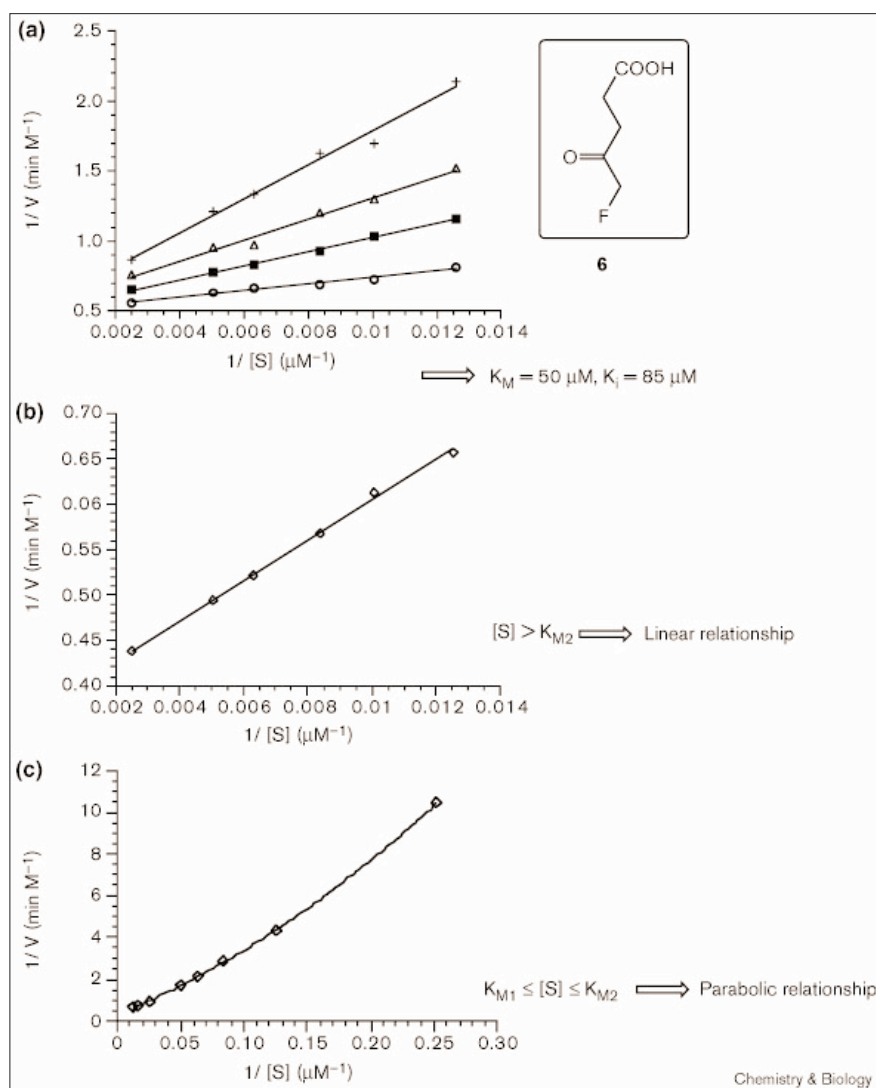
To explain the kinetic behavior of *E. coli* PBGS, the Michaelis constants of each part of the active site were needed. We calculated these values employing the

**Figure 3**

Kinetic studies of the formation of PBG catalyzed by *E. coli* PBGS. (a) The Lineweaver–Burk plot shows the results of the inhibition test using 5-fluorolevulinic acid (**6**) as an inhibitor. The plot is characteristic of competitive inhibition. The  $K_M$  and  $K_i$  values deduced from these experiments are 50  $\mu\text{M}$  and 85  $\mu\text{M}$ , respectively. In (b) and (c), the inverse of the rate of PBG formation ( $1/V$  in  $\text{min M}^{-1}$ ) is plotted against the inverse of the concentration of the substrate ( $1/[S]$  in  $\mu\text{M}^{-1}$ ) for two concentration ranges. In (b) the substrate ranges from 80–400  $\mu\text{M}$ ; and in (c) it ranges from 4–80  $\mu\text{M}$ . For the higher concentration range (b) a linear relation between  $1/V$  and  $1/[S]$  is obtained as expected for a Michaelis–Menten kinetics (classical Lineweaver–Burk plot). For the lower concentration range (c) the relationship is parabolic. The graph shows the best fit to the following equation:

$$\frac{1}{V} = \frac{1}{V_{\max}} + \frac{K_{M2}}{V_{\max}} \frac{1}{[S]} + \frac{K_{M1}K_{M2}}{V_{\max}} \frac{1}{[S]^2} \quad (1)$$

The two Michaelis–Menten constants can be obtained, and are  $4.6 \pm 1.9 \mu\text{M}$  ( $K_{M1}$ ) and  $66 \pm 13 \mu\text{M}$  ( $K_{M2}$ ), respectively.



method used for the D-Ala-D-Ala ligase, another enzyme that catalyzes the joining of two identical substrates [31,32]. By working with lower concentrations of the substrate (4–80  $\mu\text{M}$ ), we were able to see a significant deviation from the linear dependence predicted by the Michaelis–Menten kinetics (Figure 3b), and the curve is best described by second-order kinetics (Figure 3c).

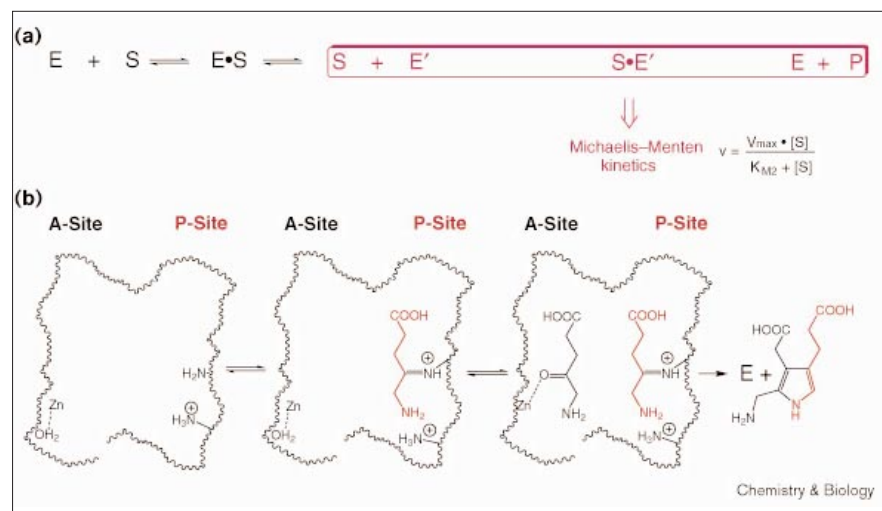
This parabolic curve could be analyzed using nonlinear regression. The kinetic model used was a steady-state model based on the sequential formation of two Michaelis complexes with two different Michaelis constants:  $K_{M1} = 4.6 \pm 1.9 \mu\text{M}$ , which corresponds to the substrate tightly bound in the P-site and  $K_{M2} = 66 \pm 13 \mu\text{M}$  for the less well bound substrate in the A-site. This last value corresponds nicely to the  $K_M$  determined under Michaelis–Menten conditions. The second order equation (see Figure 3) simplifies to a Michaelis–Menten equation (Figure 4) under standard conditions ( $[S] = 80\text{--}400 \mu\text{M}$ ). The process determining the observed enzyme kinetics is the formation of the Michaelis–Menten complex (S·E') and the formation of the final product (Figure 4) [9,24,33].

Inhibitors can interact at different steps of the reaction mechanism [33]. During our inhibition tests it became clear that significant differences in the kinetic behaviors are observed for different classes of inhibitors. Very often the inhibition behavior stays the same for a series of similar compounds. It is therefore important to determine whether the inhibition behavior differences can be explained by differences in sites of interaction in the enzyme. The large number of inhibitors studied (>121 compounds) allows us to propose a mechanistic interpretation of the differences in inhibition behavior [34,35].

Substrate and product analogs are often competitive inhibitors [25]. Competitive inhibition is attributed to a direct competition between the substrate and the inhibitor (Figure 5). Under our experimental conditions direct competition of the substrate analog inhibitors with the second substrate has to be assumed. The competitive inhibitors, therefore, have to interact with the A-site of the enzyme and all variations in their inhibition potency have to be attributed to differences in recognition of the enzyme A-site (Figure 5). The substrate analog **6** is obviously well recognized by this site.

The mechanistic interpretation of the different behaviors of some of our inhibitors (uncompetitive, irreversible, mixed or slow-binding inhibition) is less straightforward than the interpretation of the competitive behavior. We assume that inhibitors inducing more complex inhibition behaviors interact with both the A- and P-sites of the enzyme (one molecule in each site or one molecule interacting in both sites at the same time). In order for the interaction with the P-site to be kinetically relevant, the Schiff base formed between the inhibitor and the P-site lysine residue (Lys247, *E. coli* numbering) has to be more stable or at least as stable as the Schiff base formed between the substrate and Lys247. Under these conditions we will observe mixed inhibition of the free enzyme (E) and competitive inhibition with the enzyme linked with the first substrate. This double interaction leads to complex inhibition behavior; the type observed depends on the predominance of one or other of the interactions (Figure 5). Under these experimental conditions the type and the site of interaction of a specific inhibitor can be deduced from the kinetic data, interpretation of which should allow the correct reaction intermediate to be determined.

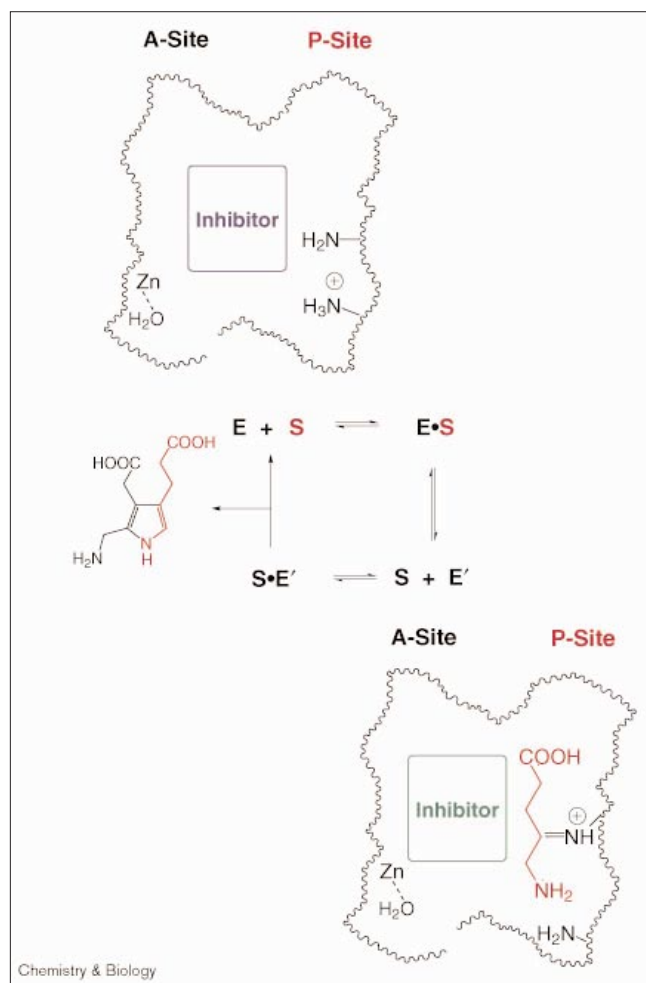
Figure 4



A kinetic scheme describing the transformation of two identical substrate molecules into one product. (a) The part of the kinetic scheme that is kinetically relevant when the concentration of the substrate is in the range of the second Michaelis–Menten constant  $K_{M2}$ . Under these conditions the P-site of the enzyme is saturated, and Michaelis–Menten kinetics are observed. (b) The different forms of the active site of the enzyme are (from left to right): E, E' and S·E.



Figure 5



A kinetic scheme of PBG biosynthesis is shown in the center. An inhibitor can interact with the free enzyme E (inhibitor in blue) or with E' where the P-side is occupied (inhibitor in green). If the inhibitor interacts, reversibly, only with the E' form, pure competitive inhibition behavior will be observed. Inhibitor interactions will result from functional groups present at the A-site of the enzyme. If the inhibitor interacts with the free enzyme E as well as with the 'mono-charged' enzyme E', the inhibition behavior will be mixed or uncompetitive depending on the relative inhibition constants at the P- and A-sites. If the inhibitor forms a stable Schiff base with the active-site lysine at the P-site, so that the release of the inhibitor becomes slow, slow-binding inhibition type will be observed. If the stability of the Schiff base between the inhibitor and the active-site lysine is so high that the inhibitor is not released any more or if a quasi-irreversible transformation follows the formation of the Schiff base (e.g. the formation of enamine tautomer, which can not be protonated on the enzyme surface) irreversible inhibition will result.

A series of diacids were tested, under conditions leading to Michaelis–Menten behavior, as potential intermediates **4** and **5** analogs (Tables 1–4). At first we tested the unfunctionalized diacids pimelic (**13**) and sebacic acids (**17**; Tables 2,3). Almost all of the simple diacids tested showed competitive inhibition behavior. The inhibition constants

Table 1

## Results of the inhibition tests of C4 analogs.

Structure	Compound	$K_i$ ( $\mu\text{M}$ )	Type of inhibition
	<b>8</b>	12,500	Competitive
	<b>9</b>	10,700	Competitive
	<b>10</b>	11,500	Competitive
	<b>11</b>	12,500	Competitive
	<b>12</b>	26,000	Competitive

See the Materials and methods section for details. The inhibition constants ( $K_i$ ) were obtained from a series of tests, in which PBGS was incubated with ALA (80–400  $\mu\text{M}$ ) and an adequate amount of the inhibitor. The amount of product PBG was measured after 14 min using Ehrlich's reagent (absorption of the chromophore  $\epsilon_{554\text{nm}} = 62,000 \text{ M}^{-1} \text{ cm}^{-1}$ ). The data were analyzed using the Lineweaver–Burk procedure to determine the inhibition type (see Figure 3). The Hanes, Eadie–Hofstee and direct plots were also analyzed, and the results from all four different methods were in good agreement. The  $K_i$  values reported were obtained from the direct plot. The  $K_M$  values obtained from the test reactions in the absence of the inhibitor were around 50  $\mu\text{M}$ . The  $K_M$  values were a good indicator of the activity and the quality of the enzyme used.

of the competitive inhibitors range from close to 10,000  $\mu\text{M}$  for fumaric acid (**9**) to > 20,000  $\mu\text{M}$  for compound **20**

Table 2







## Results of the inhibition tests of C7 analogs.

Structure	Compound	$K_i$ ( $\mu\text{M}$ )	Type of inhibition
	<b>13</b>	12,400	Competitive
	<b>14</b>	8600	Competitive
	<i>rac</i> - <b>15</b>	17,000	Competitive/activator
	<i>rac</i> - <b>16</b>	11,900	Competitive/activator

See the Materials and methods section for details. The structures of the inhibitors are drawn to imitate the proposed key intermediate **5** (see Figure 2) and the analogous intermediate that had been proposed by Shemin (see Figure 6).

Table 3

## Results of the inhibition tests of C10 analogs.

Structure	Compound	$K_i$ ( $\mu\text{M}$ )	Type of inhibition
	17	8000	Competitive/activator
	18	(-)	Irreversible
	19	(-)	Irreversible
	20	22,900	Competitive
	21	8300	Competitive
	22	(-)	Irreversible


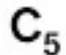

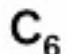

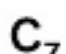

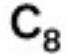
See the Materials and methods section for details. The structures of the inhibitors are drawn to imitate the proposed key intermediate **4** (see Figure 2), which would be formed as a consequence of a C–N bond between the two substrates. If an  $\gamma$ -keto function was present (as in **18** and **22**), it was drawn in the position of the P-site of the enzyme (see Figures 4 and 5). The conformation drawn for **20** is based on the knowledge that amides will not form amidines (a Schiff base analog) in the presence of amines in aqueous solution. The amide functional group was, therefore, drawn on the A-site.

(Tables 1,3). Much to our surprise there is no significant difference between fumaric acid (**9**) and maleic acid (**10**; as judged by the inhibition constants). Even the more sterically demanding phthalic acid (**11**) is in the same range of inhibition (Table 1). These competitive inhibitors show only moderate inhibition potency.

To obtain better recognition at the active site, an additional keto function was introduced to mimic more closely the postulated intermediates **4** and **5**. It is interesting to compare pimelic acid (**13**) with 4-oxo pimelic acid (**14**; Table 2). The introduction of a keto group in position 4 in pimelic acid (**13**) lowers the  $K_i$  value from 12,400  $\mu\text{M}$  to 8600  $\mu\text{M}$ . The most evident difference, however, is observed between sebacic acid (**17**) and the 4-oxo sebacic acid (**18**; Table 3). In this case the introduction of the keto function not only improved the  $K_i$  value but also changed of the type of inhibition that occurred. Sebacic acid (**17**) showed moderate competitive inhibition ( $K_i = 8000 \mu\text{M}$ ),

Table 4

## Influence of inhibitor chain length on PGBS inhibition potency.

$C_x$	Structure	Compound	$K_i$ ( $\mu\text{M}$ )	Type of inhibition
$C_5$		23	8450	Competitive
$C_6$		24	10,400	Competitive
$C_7$		14	8600	Competitive
$C_8$		25	80	Uncompetitive
$C_9$		26	450	Uncompetitive
$C_{10}$		18	(-)	Irreversible
$C_{11}$		27	(-)	Slow binder
$C_{12}$		28	(-)	Slow binder

See the Materials and methods section for details. The inhibitors that were competitive inhibitors are drawn as analogs of the substrate incorporated at the A-site of the enzyme (Figures 4,5). Inhibitors that showed uncompetitive, irreversible or slow-binding behavior are drawn in conformations that most closely resemble postulated intermediate **4** (see Figure 2). The  $\gamma$ -keto acid part of these inhibitors is always drawn in the position that corresponds to the P-site of the enzyme (Figures 4,5).

whereas the 4-oxo-sebacic acid (**18**) became an irreversible inhibitor. Other cases of irreversible inhibition were found for compounds **19** and **22** (Table 3). Even after 70 hours of dialysis the inhibitors could not be removed from the enzyme (Table 5).

Diacids with one or two more carbon atoms, such as **27** or **28**, show slow-binding inhibition and diacids with one or two fewer carbon atoms, such as **25** or **26**, are good uncompetitive inhibitors ( $K_i$  values of 80 and 450  $\mu\text{M}$ , respectively; Table 4). In the series of diacids containing ten carbon atoms, the influence of the introduction of a

Table 5

## PBGS activity after incubation with inhibitors showing time-dependent inhibition.

C <sub>x</sub>	Compound	Time-dependence of the activity		Dialysis (70 h)		Type of inhibition
		Activity (%) 30 min/90 min	Concentration (mM)	Recovery (%) after 70 h	Concentration (mM)	
C <sub>10</sub>	<b>22</b>	66/35	0.44	1	2.16	Irreversible
C <sub>10</sub>	<b>18</b>	73/32	0.41	6	6.70	Irreversible
C <sub>10</sub>	<b>19</b>	17/6	0.41	1	4.24	Irreversible
C <sub>11</sub>	<b>27</b>	84/73	0.33	28	3.26	Slow binding
C <sub>12</sub>	<b>28</b>	46/31	0.45	26	2.55	Slow binding

See the Materials and methods section for details. Enzyme activity was determined after 30 min respectively 90 min preincubation with the indicated inhibitor. Significant differences observed as a function of the preincubation time were interpreted as sign for irreversible or slow-binding inhibition. To distinguish between these two types of inhibitors, enzyme activity was determined immediately after the preincubation

second keto function (**19**), as well as one or two nitrogen atoms (**20–22**) were investigated (Table 3).

The diacids *rac*-**15** and *rac*-**16** were designed to mimic more closely the intermediate postulated by Shemin (Table 2 and Figure 6), and had showed moderate to weak competitive inhibition behavior ( $K_i$  values of 11,900  $\mu$ M and 17,000  $\mu$ M, respectively). Using lower concentrations of inhibitor and higher concentrations of ALA these compounds activated the enzyme. Testing the two diastereomers in their racemic form showed that the ratio between the inhibition constants was only 1.5. This ratio was more pronounced when these compounds were tested with *Rhodobacter spheroides* PBGS (*rac*-**15**  $K_i$  = 11,000  $\mu$ M and *rac*-**16**  $K_i$  = 25,000  $\mu$ M).

In view of obtaining compounds which could act as active-site-directed suicide inhibitors, a series of enantiomerically pure epoxides (**29**, **30**, **31** and **32**) were synthesized and tested (Figure 7). As expected, all the epoxides inhibited the enzyme irreversibly.

## Discussion

The different proposals for the PBGS mechanism postulate two structurally different key intermediates (Figure 8)

with the inhibitor and after 70 hours of dialysis. The activities were compared with the activity of PBGS preincubated in the absence of inhibitor. The % recovery of enzyme activity after dialysis is reported, showing that almost no activity was recovered for **22**, **18** and **19**. For **27** and **28** ~30% of the activity was recovered.

[3,5,9,14,23,24]. The keto diacid **14** imitates the key intermediate of the Jordan II mechanism, and the keto diacid **18** mimics the key intermediate for the Jordan I mechanism (it is three atoms longer). As our inhibitors are (structurally) highly simplified and because we do not know the importance of the other functional groups for good recognition, we decided to study a series of keto diacids (**23–28**) in addition to the keto diacids **14** and **18**, the idea being to obtain a clearer picture by analyzing the trends instead of interpreting individual inhibition constants.

If we examine the series of the diacids containing a keto function (Table 4), we can see a regular change in the behavior of these compounds with the extension of the chain length connecting the two diacids. The first derivatives **23**, **24** and **14** competitively inhibit the enzyme and we propose that they are A-site substrate analogs.

Uncompetitive inhibition is observed with the C<sub>8</sub> analog, 4-oxo suberic acid (**25**). This suggests that the inhibitor–enzyme interaction occurs at both the A- and P-sites simultaneously. We can imagine that the chain is long enough to allow interaction at the two sites, which means that recognition of the two acid functions and formation of the Schiff base could occur at the same time. This hypothesis of a

Figure 6

Comparison of the two diastereomeric diacids *rac*-**15** and *rac*-**16** with the intermediate initially postulated by Shemin, which closely resembles intermediate **5** (see Figure 2). The aldol-type reaction (C–C bond formation) that would lead to this intermediate will create two chiral centers. Because an enzyme-catalyzed reaction should follow a diastereoselective pathway, studying inhibitors that vary the relative configuration of these two centers should help to unravel the stereochemical features of this enzymatic pathway.

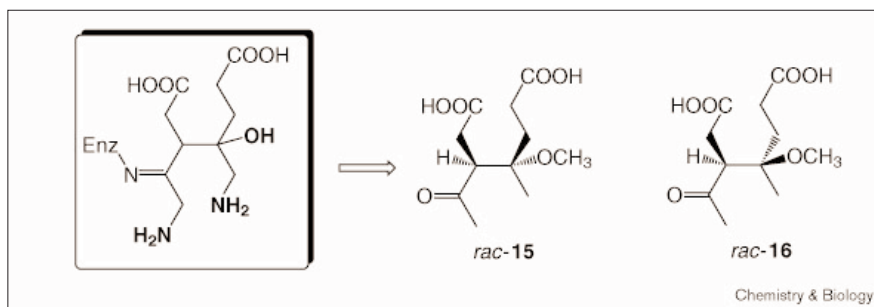
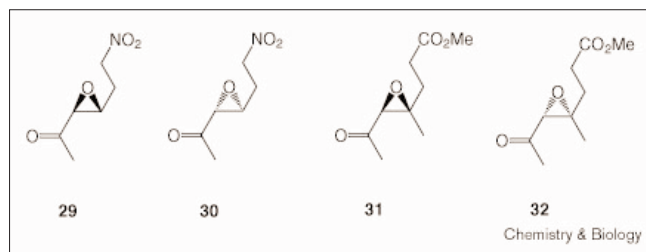


Figure 7



The enantiomerically pure inhibitors **29–32** were synthesized and studied to examine the enantioselectivity of the PBG biosynthetic pathway. At the same time the epoxy function was incorporated in order to trap nucleophiles at the active site of PBGS.

better fixation of the inhibitor when the length of the chain increases is supported by the following results. The compound 4-oxo azelaic acid (**26**) is an uncompetitive inhibitor with inhibition potency comparable to **25**. At the moment we can not unequivocally interpret the slight increase in the  $K_i$  value. The compound 4-oxo-sebacic acid (**18**) inhibits the enzyme irreversibly. This inhibitor contains the  $\gamma$ -keto carboxylic acid unit required for the formation of the Schiff base at the P-site, as well as a second carboxylic acid function that can interact with the corresponding surface at the A-site. **18** has the optimal chain length deduced from the first mechanism postulated by Jordan. The  $C_{11}$  (**27**) and  $C_{12}$  (**28**) analogs are also well recognized by the enzyme but in these cases, the inhibitors could be removed from the enzyme by dialysis and are therefore described as slow-binding inhibitors.

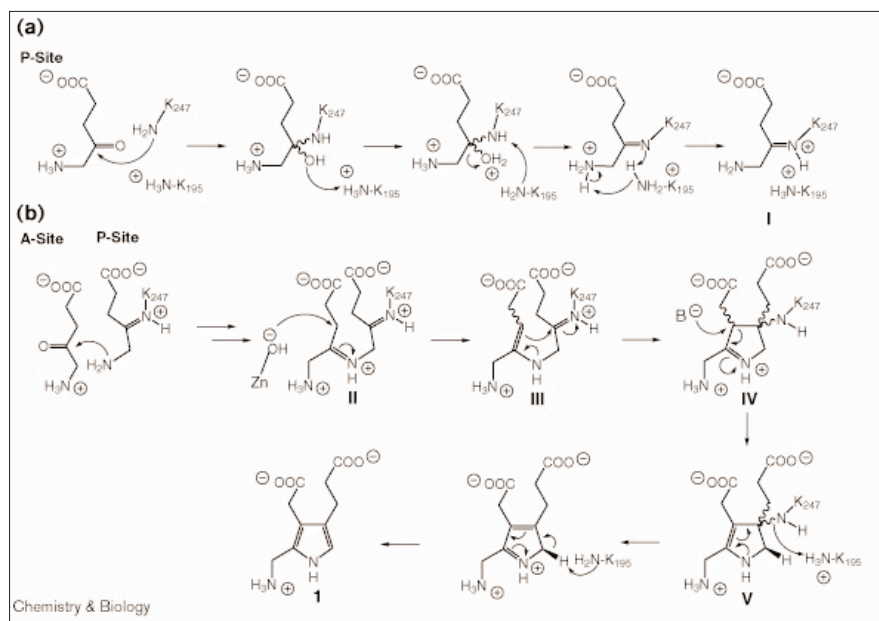
The most important result of this series is the significant inhibition difference between 4-oxo pimelic acid (**14**) and 4-oxo sebacic acid (**18**), which are structurally related to the intermediates postulated in the two different mechanisms. To reinforce the results obtained from the series of keto diacids, we decided to study compounds that more closely resembled the postulated intermediates.

We initially studied the diacids *rac*-**15** and *rac*-**16** (Figure 6) because they were close analogs of the intermediate proposed by Shemin. The amino groups had been left out in order to avoid unwanted side reactions, and the methoxy group was a consequence of the synthetic method used. The incorporation of the methoxy substituent induces at least two disadvantages: the polarity is reduced compared with the alcohol and the methoxy group clearly introduces additional steric hindrance at a sensitive site of the enzyme–intermediate complex.

The two possible diastereomers were tested separately using *R. spheroides* and *E. coli* PBGSs and showed moderate to weak competitive inhibition behavior. Despite the more close resemblance of *rac*-**15** and *rac*-**16** to the intermediate postulated by Shemin, their inhibition potency was diminished compared to the 4-oxopimelic acid (**14**).

Two conclusions can be drawn from comparing the inhibition results of the series of diacids separated by eight atoms (**17–22**; Table 3). Diacids that do not have a keto function at one of the  $\gamma$  positions of the carboxylic acids are only moderately active competitive inhibitors (**17**, **20** and **21**). Replacing the keto function of the analog of

Figure 8



Mechanism proposed for the  $Zn^{2+}$ -containing PBGSs (see text for more details).

(a) A proton shuttle role is assigned to the second lysine (Lys195) at the active site. Lys195 is also thought to be involved in the formation of the Schiff base between the first substrate and the enzyme, which is required for the bond-forming process between the two substrates. (b) The postulated involvement of Lys195 in the elimination of Lys247 from the enzyme–substrate complex and in the final aromatization, which recreates the enzyme in its native state (Lys247 neutral and Lys195 in its protonated form) is shown.  $Zn^{2+}$  might act as a Lewis acid (not formulated) in order to receive the hydroxyl group (II) and then as a base (II→III). The nature and the recreation of the base ( $B^-$ ) required for IV→V reaction is not yet clear.



intermediate **18** by an amide yields the weakest inhibitor of the whole series. The amide function will not form a Schiff base with the active-site lysine. The lack of reactivity of the carbonyl group allows us to rationalize easily the reduced inhibition potency and the different inhibition behavior.

Inhibitors **29**, **30**, **31** and **32** were synthesized and tested to try and irreversibly trap reactive sidechains at the active site of the enzyme. To induce the aldol-type reaction, double activation by a Lewis acid on the P-site and by a base on the A-site seems to be reasonable. This combination of active groups would be ideally suited to activating an epoxy group. All compounds showed a moderate time-dependent inhibition. The relatively weak inhibition of these compounds can be interpreted as the consequence of an unfavorable arrangement of the functional groups or of a weak recognition of these inhibitors at the active site.

On the basis of our inhibition results and incorporating the information from the X-ray structures [17–20], the following mechanism can be proposed for PBGS (Figure 8).

The formation of the Michaelis–Menten complex between the carbonyl of the substrate and Lys247 at the P-site of the enzyme is the first step. As shown by Shoolingin-Jordan and coworkers [17], a second lysine (Lys195) in the active site seems to be important for the formation of the Schiff base (**I**; Figure 8a). In this mechanistic proposal, we assign a proton donor or acceptor role to Lys195 during formation of the Schiff base. Then the second substrate joins the complex, forming the second Michaelis–Menten complex at the A-site. At this stage, formation of the carbon–nitrogen bond between the two substrates occurs via a Schiff base (**II**; Figure 8b). The Schiff base has to be transformed into enamine **III** for carbon–carbon bond formation to take place. The exact conformation of the intermediate required to activate the aldol-type reaction is not known. To bring the nucleophilic and electrophilic centers close enough together for the bond-forming process, the two halves of the molecule have to be twisted considerably to allow a sufficient overlap between the active centers of the enamine at the A-site and the iminium ion at the P-site. Deprotonation to the iminium ion **IV** forming the enamine **V**, followed by elimination of the amino group of the active-site Lys247 and by deprotonation (possibly by Lys195) seems to be a plausible sequence leading to porphobilinogen (**1**).

## Significance

Porphobilinogen synthase (PBGS) is an important enzyme involved in the biosynthesis of tetrapyrrolic cofactors. PBGS catalyzes the joining of two molecules of 5-aminolevulinate (ALA) by forming a carbon heteroatom bond as well as a carbon–carbon bond. Uncatalyzed dimerization of ALA leads, in most cases,

to a different product. It is important, therefore, to understand in detail the mechanism that distinguishes the biosynthetic reaction from the chemical transformation. One of the central questions is whether C–C or C–N bond formation occurs first.

The PBGS active site is composed of two sites where the two substrates bind. Using kinetic studies, we were able to estimate the Michaelis constants for each site, which were 4.6  $\mu\text{M}$  for the P-site ( $K_{M1}$ ) and 66  $\mu\text{M}$  for the A-site ( $K_{M2}$ ). We examined the kinetic behavior of PBGS systematically using different classes of inhibitors. Substrate analogs are competitive inhibitors that compete directly with binding of the second substrate at the A-site. Inhibitors that interact with both the A- and P-sites of the enzymes have more complex kinetic behavior. We studied series of carboxylic diacids to learn more about the factors responsible for substrate recognition at the active site of PBGS. An interesting chain-length dependence was observed in a series of homologous  $\gamma$  ketodiacids. Starting with keto glutaric acid, the inhibition changed from competitive to uncompetitive for keto suberic and keto azelaic acid and changed again to irreversible for keto sebacic acid. Slow-binding inhibition was observed for the longest homologs.  $\gamma$ -Keto sebacic acid is the unique irreversible inhibitor in this series. These results allowed us to define a new class of irreversible inhibitors of the *Escherichia coli* PBGS. These inhibitors are carboxylic diacids separated by eight atoms that contain at least one keto function in the  $\gamma$  position of one acid functional group. With respect to the PBGS mechanism, our results strongly support the Jordan I mechanism (shown in Figure 2), in which C–N bond formation occurs first.

## Materials and methods

### Chemistry

Chemicals (Fluka or Aldrich) and solvents (Fluka, puriss) were used without further purification. Proton magnetic resonance spectra: Bruker AMX-400 ( $^1\text{H}$ : 400 MHz,  $^{13}\text{C}$ : 100 MHz), Bruker AM 360 ( $^1\text{H}$ : 360 MHz,  $^{13}\text{C}$  90 MHz); chemical shifts  $\delta$  are reported in ppm relative to tetramethylsilane; coupling constant  $J$  in Hz; solvent  $\text{CDCl}_3$ . EI-MS (70 eV): Nermag RC 30-10. FAB-MS (glycerine, Argon): VG Micromass 7070 E. HR-MS: Bruker FTMS 4.7T BioAPEX II (ESI(positive)-MS).  $[\alpha]$ : Jasco J-710 spectropolarimeter. Elemental analyses were performed by the Microanalytical Laboratory of Ciba-Specialties SA, Marly (Switzerland). For flash column chromatography (FCC) carried out at  $\sim 0.2$  bar, silica gel 60 (0.04–0.063 mm; Fluka) was used.

### Tested compounds

Succinic acid (**8**), fumaric acid (**9**), maleic acid (**10**), phthalic acid (**11**), 2-nitrobenzoic acid (**12**), 2-oxoglutaric acid (**23**), 3-oxoadipic acid (**24**), pimelic acid (**13**), 4-oxopimelic acid (**14**), and sebacic acid (**17**) are commercially available. 4-oxosebacic acid (**18**) [36,37], 4,7-dioxosebacic acid (**19**) [38] and *N,N'*-disuccinylhydrazine (**21**) [39] were synthesized according to the literature and their spectroscopic data were consistent with previous reports. *N*-succinyl-5-aminolevulinic acid (**22**) [40] was obtained by hydrogenolysis of the corresponding dibenzyl ester synthesized by coupling of monobenzyl succinate with benzyl 5-aminolevulinatyl tosylate salt. 4-oxosuberic acid (**25**) [41] and 4-oxoazelaic acid (**26**) [42] were obtained by acid or base hydrolysis of the corresponding diesters.

Those diesters [37,43] were synthesized by the coupling of the respective organozinc ester with 3-methoxycarbonylpropionyl chloride following a procedure of Rieke and co-workers [44,45]. 4-oxoundecandioic acid (**27**) [46] and 4-oxododecandioic acid (**28**) [47] were obtained by acid hydrolysis of the corresponding diesters. Those diesters [48] (ethyl 10-methoxycarbonyl-4-oxodecanoate 92% (GC), HR-MS ( $C_{14}H_{24}NaO_5$ ): 295.1514 (calc'd 295.1516) were synthesized by alkylation and acylation of dibenzyl malonate with ethyl bromoacetate and the respective acyl chloride methyl ester then hydrogenolysis and decarboxylation in analogy to the procedure of Naora *et al.* [49].

(*rac*)-(3*R*,4*S*)-3-acetyl-4-methoxy-4-methylpimelic acid (**16**). Following the procedure of Bertschy *et al.* [50] for the Mukaiyama aldol coupling [51] of methyl 4-trimethylsilyloxy-3-pentenoate [50] and methyl levulinate dimethylacetal [52] led to 75% yield of the diastereoisomeric mixture (the ratio of (*rac*)-*RR*-**15**:(*rac*)-*RS*-**16** diesters was 1.7:1). Diastereoisomers were separated by FCC (hexane-ethyl acetate 4:1) yielding 39% of (*rac*)-*RR*-**15** diester and 17% of (*rac*)-*RS*-**16** diester.

Hydrolysis of (*rac*)-*RS*-**16** diester (1.4 g, 5.1 mmol) was undertaken in a 2:1 mixture of aqueous NaOH 0.5 M/THF (150 ml) for 3 h at room temperature. The reaction mixture was extracted once with diethylether (80 ml) then acidified with 4 M HCl to pH 2, saturated with NaCl and extracted with diethylether (6 × 100 ml). The organic layers were washed once with brine, dried over  $MgSO_4$  and evaporated. The crude product (1.3 g) was crystallized in THF/hexane to yield 760 mg (61%) of white solid product. M.p. 92–93°C. IR (KBr) 3600–2300s (br.), 1715s, 1435s, 1405s, 1380s, 1360s, 1350s, 1300s, 1250s, 1215m, 1170s, 1130s, 1120s, 1090m, 1065m, 975m, 925m, 880m.  $^1H$ -RMN  $\delta$  3.40 (dd,  $^3J$  11.4,  $^3J$  2.8, 1H, HC(3)), 3.21 (s, 3H,  $H_3CO$ ), 2.93 (dd,  $^2J$  17.6,  $^3J$  11.4, 1H, HC(2)), 2.54 (dd,  $^2J$  17.6,  $^3J$  2.8, 1H, HC(2)), 2.49–2.38 (m, 2H,  $H_2C(6)$ ), 2.32 (s, 3H, Ac), 1.94 (ddd,  $^2J$  14.7,  $^3J$  9.7,  $^3J$  5.8, 1H, HC(5)), 1.75 (ddd,  $^2J$  14.7,  $^3J$  10.0,  $^3J$  6.2, 1H, HC(5)), 1.13 (s, 3H,  $H_3CC(4)$ ).  $^{13}C$ -RMN 209.9 C(4), 179.5, 178.6 C(1), C(7), 76.5 C(4), 52.8 C(3), 49.0  $CH_3O$ , 32.8  $CH_3(Ac)$ , 32.4 C(2), 30.8 C(6), 28.1 C(5), 19.8  $CH_2C(4)$ . FAB-MS 249 (1), 248 (3), 247 (18, [M+H]<sup>+</sup>), 215 (10), 197 (8), 155 (40), 137 (28), 131 (55), 127 (30), 109 (19), 99 (100), 85 (45), 71 (16), 55 (19), 43 (100). Anal. calc'd for  $C_{11}H_{18}O_6$  (246.26): C 53.65, H 7.37; found: C 53.71, H 7.32. The same conditions were used for the hydrolysis of the major diastereoisomers.

(3*R*,4*S*)-3,4-epoxy-6-nitro-2-hexanone (**30**). Using Sharpless epoxidation conditions [53,54] on (*rac*)-6-bromo-3-hexen-2-ol, (*SSS*)-6-bromo-3,4-epoxy-2-hexanol was obtained in 29% yield and was converted by Swern oxidation in (*3R,4S*)-6-bromo-3,4-epoxy-2-hexanone in 74% yield [55].

A suspension of (*3R,4S*)-6-bromo-3,4-epoxy-2-hexanone (158 mg, 0.82 mmol) and  $AgNO_2$  (163 mg, 1.06 mmol) in hexane (20 ml) was refluxed for 3 h. The reaction mixture was filtered and the filtrate evaporated. The crude product (114 mg) was purified by FCC (heptane-ethyl acetate 4:1) to yield 64 mg (49%). IR (film) 3013w, 2924w, 1713s, 1555s, 1434m, 1381s, 1363s, 1252m, 871m, 758m.  $^1H$ -RMN  $\delta$  4.55 (ddd,  $^2J$  13.8,  $^3J$  8.2,  $^3J$  5.6, 1H, HC(6)), 4.54 (dt,  $^2J$  13.8,  $^3J$  6.3, 1H, HC(6)), 3.28–3.24 (m, 2H, HC(3), HC(4)), 2.53 (dddd,  $^2J$  15.2,  $^3J$  7.9,  $^3J$  6.5,  $^3J$  4.1,  $^4J$  1.4, 1H, HC(5)), 2.15 (dq,  $^2J$  15.2,  $^3J$  6.1, 1H, HC(6)), 2.09 (s, 3H,  $H_3C(1)$ ).  $^{13}C$ -RMN 205.0 C(2), 72.1 C(6), 59.9 C(3), 55.0 C(4), 29.8 C(5), 25.3 C(1). EI-MS 160 (<1, [M+H]<sup>+</sup>), 159 (<1, [M]<sup>+</sup>), 116 (19), 85 (9), 43 (100), 41 (19), 30 (11).  $[\alpha]_D^{298} = +14.22^\circ$  ( $CH_2Cl_2$ ,  $c = 0.696$ ). Anal. calc'd for  $C_6H_9NO_4$  (159.14): C 45.28, H 5.70, N 8.80; found: C 44.72, H 5.63, N 9.25.

Methyl (4*S*,5*R*)-epoxy-4-methyl-6-oxooctanoate (**32**). Starting from the geraniol, (4*S*,5*R*)-epoxy-4-methyl-6-oxooctanal was obtained by Sharpless epoxidation followed by Swern oxidation of the alcohol function, attack of the resulting aldehyde with MeLi, then Swern oxidation and finally by ozonolysis of the double bond with an overall yield of 28% [55].

A solution of (4*S*,5*R*)-epoxy-4-methyl-6-oxooctanal (1.02 g, 6.56 mmol) in methanol (1.26 g, 39.4 mmol) was stirred at room temperature for

15 min. DMF (20 ml) and PDC (14.8 g, 39.4 mmol) were added (water bath cooling) and the reaction mixture was stirred 18 h at room temperature before being worked up with water (300 ml) and extracted with ethyl acetate (6 × 50 ml). The organic layers were washed with 0.1 M HCl (200 ml), 1%  $NaHCO_3$  (200 ml), dried over  $MgSO_4$ , filtered and evaporated to yield 668 mg (55%) of liquid product. IR (film) 2955m, 1738s, 1439m, 1407m, 1386m, 1359m, 1297m, 1195s, 1089m, 840m.  $^1H$ -RMN  $\delta$  3.69 (s, 3H,  $H_3CO$ ), 3.42 (s, 1H, HC(5)), 2.41 (t,  $^3J$  7.6, 2H, HC(2)), 2.21 (s, 3H,  $H_3C(7)$ ), 2.00 (dt,  $^2J$  14.3,  $^3J$  7.2, 1H, HC(3)), 1.99 (dt,  $^2J$  14.3,  $^3J$  7.9, 1H, HC(3)), 1.25 (s, 3H,  $H_3CC(4)$ ).  $^{13}C$ -RMN 204.6 C(6), 173.6 C(1), 65.1 C(5), 62.9 C(4), 52.5  $CH_3O$ , 33.4 C(3), 30.0 C(2), 28.6 C(7), 17.0  $CH_2C(4)$ . EI-MS 187 (100, [M+H]<sup>+</sup>), 169 (16), 155 (6), 145 (15), 127 (10), 113 (9), 99 (15). Anal. calc'd for  $C_9H_{14}O_4$  (186.21): C 58.05, H 7.58; found: C 57.81, H 7.63.

#### Materials

*E. coli* (CR 261) was a gift from C. Roessner of Texas A&M University. Production of *E. coli* and purification of PBGS have been described previously [15].

#### PBGS assay and determination of kinetic constants

The PBGS assay is a colorimetric assay based on the reaction between PBG and 4-dimethylaminobenzaldehyde [56], the so-called Ehrlich's reagent.

The assay for *E. coli* PBGS contained 4–6.4  $\mu g$  PBGS, the inhibitor in 1.5 ml of 0.1 M NaP ( $NaH_2PO_4$ - $Na_2HPO_4$  mixture) (pH = 8.1, 12.3 mM mercaptoethanol, 10 mM  $MgCl_2 \cdot 6H_2O$  and 10  $\mu M$   $ZnCl_2$ ). The preincubation took place at 37° for 30–45 min. The substrate was added in varying concentrations and the solution was incubated for 14 min, after which the PBGS-catalyzed reaction was stopped by adding 1 ml of the stop reagent (20% TCA, 10 mM  $HgCl_2$ ) at 0°C. After centrifugation (4 min, 3600 g) 1 ml of the supernatant was treated with 1 ml of Ehrlich's reagent (4-dimethylaminobenzaldehyde in perchloric acid 70%/acetic acid solution). This solution was centrifuged (4 min, 3,600 g) for a second time. The quantity of product formed was determined by measuring the absorbance at 554 nm ( $\epsilon = 62,000$  [mol<sup>-1</sup> cm<sup>1</sup>]).

The type of inhibition was determined using Eadie–Hofstee, Lineweaver–Burk and Hanes plots. The  $K_i$  values shown in the different tables are the average of at least three independent assays.  $K_i$  values were calculated from the apparent  $K_M$  deduced from the hyperbolic plot, typical for Michaelis–Menten kinetics.

#### Calculation of the kinetic constants $K_{M1}$ and $K_{M2}$

400  $\mu l$  of a solution containing 1.1 mg of PBGS diluted in 70 ml of phosphate buffer (0.1M NaP, at pH = 8.1, 12.3 mM mercaptoethanol, 10 mM  $MgCl_2 \cdot 6H_2O$  and 10  $\mu M$   $ZnCl_2$ ) was added to (1100–X)  $\mu l$  of phosphate buffer (X = 20, 40, 60, 80, 100, 200, 300 or 400  $\mu l$ ). The different tubes were preincubated 15 min at 37°. After addition of X  $\mu l$  of ALA solution (0.5 mg/ml for assay (a) and 0.05 mg/ml for assay (b)), the tubes are incubated for 14 min. The PBGS-catalyzed reaction was then stopped by adding 1 ml of the stop reagent at 0°C. After centrifugation (4 min, 3600 g) 1 ml of the supernatant was treated with 1 ml of Ehrlich's reagent. This solution was centrifuged (4 min, 3,600 g) for a second time. The quantity of product formed was determined by measuring the absorbance at 554 nm ( $\epsilon = 62,000$  [mol<sup>-1</sup> cm<sup>1</sup>]; Table 5).

The Lineweaver–Burk plot (1/v against 1/[S]) was used to deduce the two Michaelis constants of each site using nonlinear regression (see Figure 3).

#### Estimation of the specific activity

Protein concentration was estimated by the Bio-Rad Protein Assay using the color change of the Coomassie Brilliant Blue-G-250. This color change is followed by measuring the absorbance at 596 nm [57]. The concentration of our protein is deduced by comparison with a standard curve. Using this value together with the rate of PBG formation allows the specific activity to be calculated.

**Table 6****Determination of the two Michaelis constants  $K_{M1}$  and  $K_{M2}$** (a) Concentration of 5-aminolevulinic acid between 80 and 400  $\mu\text{M}$ .

Concentration of ALA ( $\mu\text{M}$ )	Absorbance	Rate ( $\mu\text{M min}^{-1}$ )
79.58	0.396	1.522
99.48	0.425	1.632
119.37	0.459	1.762
159.16	0.500	1.920
198.95	0.526	2.022
397.91	0.595	2.285

(b) Concentration of 5-aminolevulinic acid between 4 and 80  $\mu\text{M}$ .

Concentration of ALA ( $\mu\text{M}$ )	Absorbance	Rate ( $\mu\text{M min}^{-1}$ )
3.97	0.025	0.096
7.95	0.060	0.230
11.91	0.091	0.349
15.89	0.124	0.476
19.85	0.152	0.584
39.70	0.288	1.106
59.55	0.358	1.375
74.40	0.412	1.582

Figures 3b,c present these results graphically. The rate ( $v$ ) is calculated using the following equation:  

$$v = (n [\text{factor dilution}] \cdot \text{Abs} \cdot 10^6) / (e \cdot l [\text{cell length}] \cdot t [\text{incubation time}])$$

**Dialysis assay**

4–6.4  $\mu\text{g}$  PBGS were dissolved in 10 ml phosphate buffer (0.1M NaP, pH = 8.0, 12.3 mM mercaptoethanol, 10 mM  $\text{MgCl}_2 \cdot 6\text{H}_2\text{O}$  and 10  $\mu\text{M}$   $\text{ZnCl}_2$ ). 4 ml of this solution was placed in two different 5 ml tubes, one containing 5.8 mg of 4-oxo-sebacic acid (**19**) and the second (without inhibitor) was used as a reference. After 24 h at room temperature, the specific activities were determined. The solution containing the inhibitor showed only 22.4% of the specific activity compared to the blank experiment. 1 ml of each solution was placed in a dialysis tube and separately dialyzed against 2.5 l phosphate buffer solution (0.1M NaP, pH = 8.0, 12.3 mM mercaptoethanol, 10 mM  $\text{MgCl}_2 \cdot 6\text{H}_2\text{O}$  and 10  $\mu\text{M}$   $\text{ZnCl}_2$ ). After 66 h dialysis at 4°C, the specific activities were again determined (the solution initially containing the inhibitor showed 28.5% of the specific activity compared to the blank experiment). The same measurements were repeated with compounds **19**, **22**, **27** and **28** (Table 6).

**Acknowledgements**

We thank the Swiss National Science Foundation and the Foundation of the Basel Chemical Industry for financial support of our work.

**References**

- Battersby, A.R., Fookes, C.J.R., Matcham, G.W.J. & McDonald, E. (1980). Biosynthesis of the pigments of life: formation of the macrocycle. *Nature* **285**, 17-21.
- Shemin, D. (1970).  $\delta$ -Aminolevulinic acid dehydratase (*Rhodospseudomonas spheroides*). *Methods Enzymol.* **XVII Part A**, 205-211.
- Cheh, A.M. & Neilands, J.B. (1976). The  $\delta$ -aminolevulinic acid dehydratase: molecular and environmental properties. In *Bonding and Structure*. pp.123-169, Springer-Verlag, Berlin.
- Leeper, F.J. (1989). The biosynthesis of porphyrins, chlorophylls and vitamin B<sub>12</sub>. *Nat. Prod. Rep.* **6**, 171-203.
- Jordan, P.M. (1991). The biosynthesis of 5-aminolevulinic acid and its transformation into uroporphyrinogen III. In *Biosynthesis of Tetrapyrroles*. (Jordan, P.M., ed.) pp.1-66, Elsevier, Amsterdam.
- Franck, B. & Stratmann, H. (1981). Condensation products of the porphyrin precursor 5-aminolevulinic acid. *Heterocycles* **15**, 919-923.
- Scott, I.A., Townsend, C.A., Okada, K. & Kajiwara, M. (1973). Concerning the biosynthesis of vitamin B<sub>12</sub>. *Trans. N.Y. Acad. Sci.* **35**, 72-79.
- Butler, A.R. & George, S. (1992). The nonenzymatic cyclic dimerisation of 5-aminolevulinic acid. *Tetrahedron* **48**, 7879-7886.
- Neier, R. (1996). Chemical synthesis of porphobilinogen and studies of its biosynthesis. In *Advances in Nitrogen Heterocycles*. (Moody, C.J. ed.) pp.35-146, JAI Press Inc., Greenwich, Connecticut.
- Nandi, D.L. & Shemin, D. (1968).  $\delta$ -Aminolevulinic acid dehydratase of *Rhodospseudomonas spheroides*. II. Association to polymers and dissociation to subunits. *J. Biol. Chem.* **243**, 1231-1235.
- Echelard, Y., Dymetryszyn, J., Drolet, M. & Sasarman, A. (1988). Nucleotide sequence of the *hemB* gene of *Escherichia coli* K12. *Mol. Gen. Genet.* **214**, 503-508.
- Jaffe, E.K. (1995). Porphobilinogen synthase, the first source of heme's asymmetry. *J. Bioenerg. Biomembr.* **27**, 169-179.
- Gibbs, P.N.B. & Jordan, P.M. (1986). Identification of lysine at the active site of human 5-aminolevulinic acid dehydratase. *Biochem. J.* **236**, 447-451.
- Nandi, D.L. & Shemin, D. (1968).  $\delta$ -Aminolevulinic acid dehydratase of *Rhodospseudomonas spheroides*, III. Mechanism of porphobilinogen synthesis. *J. Biol. Chem.* **243**, 1236-1242.
- Mitchell, L.W. & Jaffe, E.K. (1993). Porphobilinogen synthase from *Escherichia coli* is a Zn(II) metalloenzyme stimulated by Mg(II). *Arch. Biochem. Biophys.* **300**, 169-177.
- Petrovich, R.M., Litwin, S. & Jaffe, E.K. (1996). *Bradyrhizobium japonicum* porphobilinogen synthase uses two Mg(II) and monovalent cations. *J. Biol. Chem.* **271**, 8692-8699.
- Erskine, P.T., *et al.*, & Cooper, J.B. (1997). X-ray structure of 5-aminolevulinic acid dehydratase, a hybrid aldolase. *Nat. Struct. Biol.* **4**, 1025-1031.
- Erskine, P.T., *et al.*, & Cooper, J.B. (1999). The Schiff base complex of yeast 5-aminolevulinic acid dehydratase with laevulinic acid. *Protein Sci.* **8**, 1250-1256.
- Erskine, P.T., *et al.*, & Shoolingin-Jordan, P.M. (1999). X-ray structure of 5-aminolevulinic acid dehydratase from *Escherichia coli* complexed with the inhibitor levulinic acid at 2.0 Å resolution. *Biochemistry* **38**, 4266-4276.
- Frankenberg, N., Erskine, P.T., Cooper, J.B., Shoolingin-Jordan, P.M., Jahn, D. & Heinz, D.W. (1999). High resolution crystal structure of a Mg<sup>2+</sup> dependent porphobilinogen synthase. *J. Mol. Biol.* **289**, 591-602.
- Sundberg, R.J. (1996). Pyrroles and their benzo derivatives: synthesis. In *Comprehensive Heterocyclic Chemistry*. (Katritzky, A.R., Rees, C.W. & Scriven, E.F. eds) pp. 275-321, Elsevier Science Ltd., Oxford, UK.
- Abeles, R.H., Frey, P.A. & Jencks, W.P. Nitrogen metabolism: amino acids, urea, and heme. In *Biochemistry*. (pp.714-717), Jones and Bartlett Publishers, Boston.
- Jordan, P.M. & Seehra, J.S. (1980). Mechanism of action of 5-aminolevulinic acid dehydratase: stepwise order of addition of the two molecules of 5-aminolevulinic acid in the enzymic synthesis of porphobilinogen. *J. Chem. Soc. Chem. Commun.*, 240-242.
- Granick, S. & Mauzerall, D. (1958). Porphyrin biosynthesis in erythrocytes. II. Enzymes converting  $\delta$ -aminolevulinic acid to coproporphyrinogen. *J. Biol. Chem.* **232**, 1119-1140.
- Lüönd, R.M., Walker, J. & Neier, R.W. (1992). Assessment of the active-site requirements of 5-aminolevulinic acid dehydratase: Evaluation of substrate and product analogues as competitive inhibitors. *J. Org. Chem.* **57**, 5005-5013.
- Senior, N.M., *et al.*, & Warren, M.J. (1996). Comparative studies on the 5-aminolevulinic acid dehydratases from *Pisum sativum*, *Escherichia coli* and *Saccharomyces cerevisiae*. *Biochem. J.* **320**, 401-412.
- Cheung, K-M., Spencer, P., Timko, M.P. & Shoolingin-Jordan, P.M. (1997). Characterization of a recombinant pea 5-aminolevulinic acid dehydratase and comparative inhibition studies with the *Escherichia coli* dehydratase. *Biochemistry* **36**, 1148-1156.
- Appleton, D., Duguid, A.B., Lee, S-K., Ha, Y-J., Ha, H-J. & Leeper, F.J. (1998). Synthesis of analogues of 5-aminolevulinic acid and inhibition of 5-aminolevulinic acid dehydratase. *J. Chem. Soc. Perkin. Trans.* **1**, 89-101.
- Cornish-Bowden, A. & Wharton, C.W. (1990). Reactions of two substrates. In *Enzyme Kinetics*. (Rickwood, D. & Male, D. eds), pp.25-33, IRL Press Limited, Oxford.



30. Michaelis, M. & Menten, M.L. (1913). Die kinetik der invertinwirkung. Kinetics of the action of invertine [Kinetics of the action of invertine]. *Biochem. Z.* **49**, 333-369.
31. Neuhaus, F.C. (1962). The enzymatic synthesis of D-alanyl-D-alanine. *J. Biol. Chem.* **237**, 3128-3135.
32. Zawadzke, L.E., Bugg, T.D.H. & Walsh, C.T. (1991). Existence of two D-alanine:D-alanine ligases in *Escherichia coli*: cloning and sequencing of the *ddlA* gene and purification and characterization of the DdlA and DdlB enzymes. *Biochemistry* **30**, 1673-1682.
33. Tschudy, D.P., Hess, R.A. & Frykholm, B.C. (1981). Inhibition of  $\delta$ -aminolevulinic acid dehydrase by 4,6-dioxoheptanoic acid. *J. Biol. Chem.* **256**, 9915-9923.
34. Henz, M. (1996). Inhibitionsstudien zum mechanismus der porphobilinogen synthase isoliert aus *Escherichia coli* CR 261 [Inhibition studies of porphobilinogen synthase isolated from *Escherichia coli* 261 in view of elucidating the mechanism of PBGS] [PhD thesis]. University of Neuchâtel.
35. Jarret, C. (1999). Etude de la porphobilinogène synthase d'*Escherichia coli*: inhibition sélectives des deux sites actifs [Studies of *Escherichia coli* porphobilinogen synthase: directed site selective inhibition] [PhD thesis]. University of Neuchâtel.
36. Hünig, S. & Lücke, E. (1959). Kettenverlängerung von dicarbonsäuren um 6 und 12 C-atome. [Chain elongation of dicarboxylic acids by 6 and 12 C-atoms.] *Chem. Ber.* **92**, 652-662.
37. Zürcher, A. & Hesse, M. (1987). Die oxidation von 3-(1-nitro-2-oxocycloalkyl)propanal [Oxidation of 3-(1-nitro-2-oxocycloalkyl)propanal]. *Helv. Chim. Acta* **70**, 1937-1943.
38. Diels, O. & Alder, K. (1931). Synthesen in der hydroaromatischen reihe; 'dien-synthesen' mit pyrrol und seinen homologen [Synthesis in the field of hydrogenated aromatic rings; 'diene-synthesis' using pyrrol and its homologs]. *Justus Liebigs Ann. Chem.* **486**, 211-225.
39. Feuer, H., Bachman, G.B. & White, E.H. (1951). The reaction of succinic anhydride with hydrazine hydrate. *J. Am. Chem. Soc.* **73**, 4716-4719.
40. Neuberger, A. & Scott, J.J. (1954). The synthesis of  $\delta$ -succinamidolævulinic acid and related compounds. *J. Chem. Soc.* 1820-1825.
41. Heller, J., Yogev, A. & Dreiding, A.S. (1972). Bishomochinon. [Bishomoquinone.] *Helv. Chim. Acta* **55**, 1003-1025.
42. Kostova, K. & Hesse, M. (1984).  $\gamma$ -Nitro- $\gamma$ -butyrolacton [ $\gamma$ -Nitro- $\gamma$ -butyrolactone]. *Helv. Chim. Acta* **67**, 1725-1728.
43. Rieke, R.D., Wehmeyer, R.M., Wu, T.C. & Ebert, G.W. (1989). New organocopper reagents prepared utilizing highly reactive copper. *Tetrahedron* **45**, 443-454.
44. Zhu, L., Wehmeyer, R.M. & Rieke, R.D. (1991). The direct formation of functionalized alkyl(aryl)zink halides by oxidative addition of highly reactive zinc with organic halides and their reactions with acid chlorides,  $\alpha,\beta$ -unsaturated ketones, and allylic, aryl and vinyl halides. *J. Org. Chem.* **56**, 1445-1453.
45. Guijarro, D., Rosenberg, D.M., Rieke, R.D. (1999). The reaction of active zinc with organic bromides. *J. Am. Chem. Soc.* **121**, 4155-4167.
46. Finch, N., Fitt, J.J. & Hsu, I.H.C. (1971). Cyclopentenone synthesis by directed cyclization. *J. Org. Chem.* **36**, 3191-3196.
47. Serebryakov, E.P., Simolin, A.V., Kucherov, V.F. & Rozyrov, B.V. (1970). New metabolites of *Fusarium moniliform*. *Tetrahedron* **26**, 5215-5223.
48. Sharma, K.K. & Torsell, K.B.G. (1984). New routes to  $\gamma$ -ketoesters,  $\beta$ -hydroxy- $\delta$ -ketoesters,  $\alpha,\beta$ -unsaturated  $\gamma$ -ketoaldehydes and acetals. Synthesis of cyclopentenones. *Tetrahedron* **40**, 1085-1089.
49. Naora, H., Ohnuki, T. & Nakamura, A. (1988). An improved synthesis of methyl 7-(2-hydroxy-5-oxo-1-cyclopentenyl)heptanoate. *Bull. Chem. Soc. Jpn.* **61**, 993-994.
50. Bertschy, H., Meunier, A. & Neier, R. (1990). A new pyrrole synthesis. *Angew. Chem. Int. Ed. Engl.* **29**, 777-778.
51. Mukaiyama, T. (1982). The directed aldol reaction. *Org. React.* **28**, 203-331.
52. Meister, C. & Scharf, H.D. (1983). Synthese von (1s)-(-)-frontalin [Synthesis of (1s)-(-)-frontaline]. *Liebigs Ann. Chem.* 913-921.
53. Johnson, R.A. & Sharpless, K.B. (1991). Addition reactions with formation of carbon-oxygen bonds: (ii) Asymmetric methods of epoxidation. In *Comprehensive Organic Synthesis. Vol. 7 Oxidation*. (Trost, B.M. ed.), pp. 389-436, Pergamon Press, Oxford, UK.
54. Carlier, P.R., Mungall, W.S., Schröder, G. & Sharpless, K.B. (1988). Enhanced kinetic resolution and enzyme-like shape selectivity. *J. Am. Chem. Soc.* **110**, 2978-2979.
55. Marty, M. (1995). Synthese von enantiomerenreinen analoga eines möglichen zwischenproduktes der PBG biosynthese [Chain elongation of dicarboxylic acids by 6 and 12 C-atoms] [PhD thesis]. University of Neuchâtel.
56. Mauzerall, D. & Granick, S. (1956). The occurrence and determination of  $\delta$ -aminolevulinic acid and porphobilinogen in urine. *J. Biol. Chem.* **219**, 435-446.
57. Bradford, M.M. (1977). A rapid and sensitive method for the quantitation of microgram quantities of protein utilizing the principle of protein-dye binding. *Anal. Biochem.* **72**, 248-254.